Consideration of Deformation of TiN Thin Films with Preferred Orientation Prepared by Ion-Beam-Assisted Deposition*

Toshiyuki HAYASHI**, Akihito MATSUMURO***
Tomohiko WATANABE****, Toshihiko MORI****
Yutaka TAKAHASHI***** and Katsumi YAMAGUCHI****

Plastic deformation of TiN thin films with (111) and (200) preferred orientation was determined based on their hardness anisotropy. Hardness was measured by means of the nano-indentation technique. Plastic deformation of TiN films was caused by the indentation of the trigonal diamond tip, and evidence of this phenomenon was provided by cross-sectional scanning electron microscopy (SEM) observation and transmission electron diffraction (TED) analysis. The influence of the differences in residual stress and grain size on hardness anisotropy was restrictive, and hardness anisotropy can be explained by the anisotropy of yield stress as calculated using Schmid's law. This relationship suggests the existence of a {100}<110> slip system in the TiN crystal. Transmission electron microscopy (TEM) observation of brittle cracks in TiN films confirmed that these cracks are caused not by cleavage fractures but by intergranular fractures.

Key Words: Plasticity, Anisotropy, Hardness, Titanium Nitride, Slip System, Preferred Orientation, Ion-Beam-Assisted Deposition, Thin Film, Coating

1. Introduction

TiN is an NaCl-type crystal that has widely been used as a wear- and corrosion-resistant film on mechanical components such as tool materials and biocompatible materials due to its excellent mechanical and chemical properties such as high hardness, low wear coefficient and chemical stability. In recent years, much interest has been focused on the use of TiN films as diffusion barrier layers between Al wires and VLSI Si devices[1]. It has thus become necessary to investigate the mechanical, physical and chemical properties of TiN films in terms of their crystallographical properties such as microstructure. However, the slip system of TiN crystals, which affects their mechanical properties, has not yet been clarified while those of some NaCl-type crystals, e.g., MgO, have already been revealed[2]. One of the reasons for this is that a bulk single crystal of TiN is extremely difficult to obtain.

Recently, attempts have been made to synthesize preferentially oriented TiN thin films owing to the increasing number of applications of TiN[3]-[6]. Consequently, elastic anisotropy[2] and other types of anisotropy have gradually been investigated. However, no analysis of the slip system of TiN crystals based on the hardness anisotropy of preferentially oriented TiN thin films has been performed to date.

We previously reported the formation of strongly (111)- and (200)-oriented TiN thin films by ion-beam-assisted deposition (IBAD) with a suitable N/Ti transport ratio, N ion incidence angle and substrate temperature[7]. We also reported the hardness anisotropy of TiN by nano-indentation analysis of these

* Received 27th January, 2000. Japanese original: Trans. Jpn. Soc. Mech. Eng., Vol. 65, No. 636, A (1999), pp. 1818-1823 (Received 11th November, 1998)

** Department of Mechanical Engineering, Nagoya University, Furo, Chikusa, Nagoya 464-8603, Japan. E-mail: hayashi@upr.mech.nagoya-u.ac.jp
*** Department of Micro System Engineering, Nagoya University, Furo, Chikusa, Nagoya 464-8603, Japan
**** Department of Mechanical Engineering, Nagoya University, Furo, Chikusa, Nagoya 464-8603, Japan
***** Department of Mechanical Engineering, Mie University, Kamihama, Tsu 514-8507, Japan

Table 1 Experimental conditions for TiN thin films with preferred orientation

Preferred orientation	TiN (200)	TiN (111)
Deposition source	Ti	
Ion species	$N_2^+ + N^+$	
N ion acceleration energy (keV)	1	
N ion beam flux ($\mu A/cm^2$)	37	
Film thickness (nm)	1000	
Deposition temperature (°C)	500	< 100 (r. t.)
Deposition rate (nm/s)	0.2	1.2
Rotation speed of substrate (rpm)	3	

preferentially oriented TiN thin films[8].

In this study, the slip system of TiN crystals is investigated by comparing qualitatively experimental hardness anisotropy with calculated crystallographical anisotropy using Schmid's law[9].

2. Experimental Details

2.1 Film preparation

(111)- and (200)-oriented TiN thin films were prepared on Si (100) substrate by IBAD[8]. Experimental conditions for film formation are listed in Table 1. In what follows, (111)- and (200)-oriented TiN films are referred to as TiN (111) and TiN (200), respectively.

2.2 Film characterization

The hardness of TiN thin films was analyzed by means of the nano-indentation method (CSIRO UMIS-2000) using a trigonal diamond indenter (Berkovich type). The relationship between hardness and indentation depth was investigated based on changes in the maximum indentation load in the range of 2 to 50 mN. The hardness measured at shallower indentation depths is important due to the reduction in the effect of substrate hardness. In this study, the hardness of the obtained film was determined by extrapolation of the hardness-depth curve toward the film surface[8].

The composition of TiN films was analyzed by Auger electron spectroscopy (AES). The grain size was determined by approximation of the grain shape to a sphere after the grain shape was observed by atomic force microscopy (AFM). The residual stress was estimated by deflection measurements[10]. The effects of these parameters are discussed during the consideration of hardness anisotropy.

2.3 Microstructure of TiN films

Evidence of plastic deformation was provided by cross-sectional scanning electron microscopy (SEM) observation of the indented depression of TiN thin film with a 30 kV electron beam. This depression was cut into sections by a focused ion beam (FIB) with 30 keV Ga^+ ions. Crystal rotation at the center of the imprint caused by plastic deformation was observed by transmission electron diffraction (TED) with a 300 kV electron beam.

Table 2 Mechanical and structural properties of TiN thin films with preferred orientation[8]

Preferred orientation	TiN (200)	TiN (111)
Hardness (GPa)	15	9
Residual compressive stress (MPa)	220	80
Composition N/Ti	1.1	1.0
Grain size (nm)	32	24

Moreover, the fracture mechanism during indentation was examined by transmission electron microscopy (TEM) observation of brittle cracks at the periphery of the depressions.

3. Results and Discussion

3.1 Hardness anisotropy

Table 2 lists the hardnesses of TiN (200) and TiN (111) thin films[8]. In this table, the composition, residual stress and grain size are also described to discuss the effects of these parameters on hardness anisotropy. This table revealed the obvious anisotropy of hardness. On the other hand, the effects of composition and residual compressive stress on the hardness of TiN films were reported as 1 GPa for composition[11] and 0.2 GPa for residual stress[12]. The relationship between grain size and yield stress corresponding to hardness is well known as the Hall-Petch relation. Based on the above results, the hardness anisotropy of TiN films was considered to be caused by the crystallographical anisotropy of TiN crystals[8].

3.2 Microstructure

Figures 1 and 2 show cross-sectional SEM images of indented depressions of TiN (111) and TiN (200), respectively. The depression of TiN (111) shown in Fig. 1 was indented with a load of 50 mN for the clarification of a prominent difference in yield stress, while that of TiN (200) shown in Fig. 2 was indented with a load of 500 mN. To calculate the average of indentation stresses, the projected areas of depressions were evaluated from these figures and were then divided by the indentation loads. Table 3 lists the calculated average of indentation stresses and the anisotropy. The anisotropy of the average of indentation stress qualitatively corresponded to that of analyzed hardnesses listed in Table 2. Therefore, the relevance of the analyzed hardness anisotropy was also supported by SEM observation.

The crystal structure of TiN, i.e., NaCl type, is typically ionic with directional bonds. On the other hand, slip deformation generally occurs in metals with

Table 3 Average of the indentation stress applied to the projection of the indenter

Preferred orientation	TiN (200)	TiN (111)
Average of indentation stress (GPa)	11.2	6.2

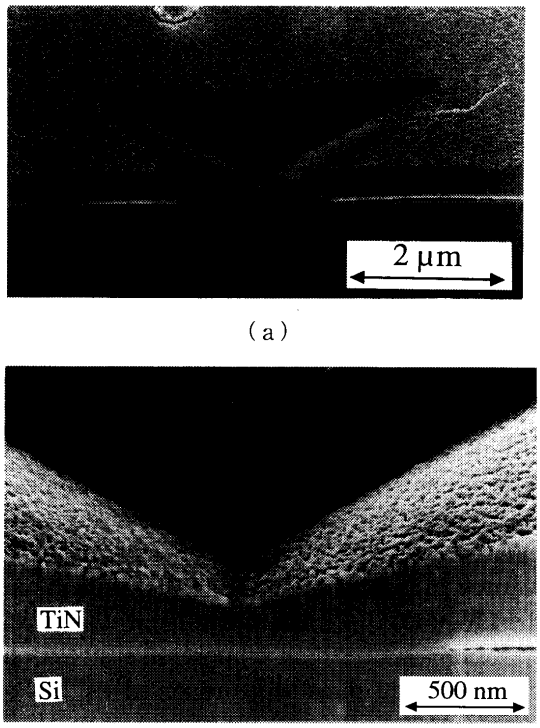

(a)

(b)

Fig. 1 Cross-sectional SEM image of TiN (111) thin film after indentation with a load of 50 mN. (b) is a magnified view of (a)

non-directional bonds. Therefore, a discussion of the occurrence of slip deformation in TiN films is indispensable.

The TiN (111) film became thin at the center of the imprint during indentation with a load of 50 mN as shown in Fig. 1, while plastic deformation was hardly observed at the Si substrate. Delamination at the interface between TiN thin film and Si substrate was observed at the periphery of the imprint. These results confirmed that the plastic flow of TiN film at the center of the imprint was caused by an indentation, and that only the quantity of flowed TiN corresponded to the indentation volume. The interface was delaminated by the compressive stress and the bending moment in TiN film at the periphery of the imprint owing to this plastic flow. On the other hand, no delamination occurred at the center of imprint, which was due to elastic recovery during unloading.

The TiN (200) film became only slightly thin and was projected during the application of an indentation load of 500 mN, as shown in Fig. 2, while obvious

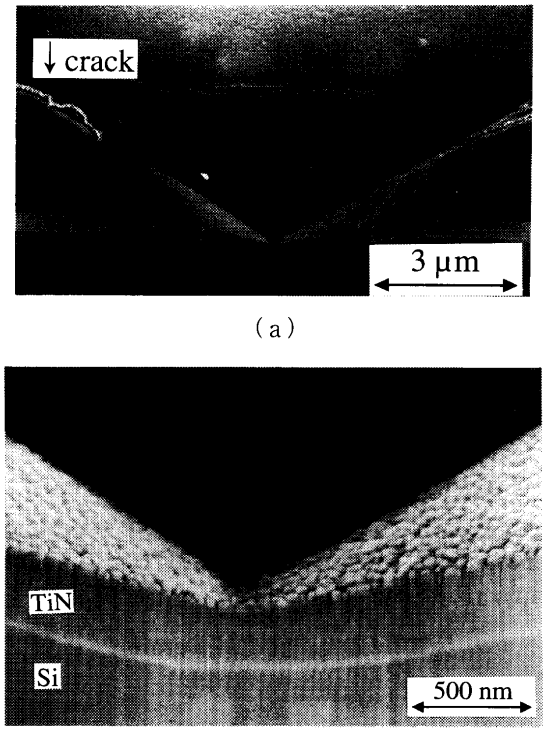

(a)

(b)

Fig. 2 Cross-sectional SEM image of TiN (200) thin film after indentation with a load of 500 mN. (b) is a magnified view of (a)

plastic deformation of the Si substrate was observed due to an indentation load ten times higher than that in Fig. 1. This phenomenon was a result of the hardness and yield stress of TiN (200) thin films which were higher than those of the Si substrate. Because the projected deformation on the macroscopic scale should be reflected in the crystal rotation on the microscopic scale, TED observation of TiN (200) was performed to confirm the existence of crystal rotation. Figure 3 shows a plane view of the TED patterns of TiN (200). This sample was prepared by etching with KOH solution to remove the substrate. Figure 3(a) shows the TED pattern measured at the periphery of the imprint. In this figure, diffraction rings corresponding to TiN (200) and (220) and arising from a (200)- oriented cubic crystal were observed clearly. Figure 3(b) shows the TED pattern measured at the center of the imprint. In this figure, diffraction rings corresponding to TiN (111) and (311) were also observed. These results show that although TiN (200) thin film was only projected during indentation, crystal rotation due to plastic deformation was still observed.

It follows from the above discussion that the hardness anisotropy of preferentially oriented TiN thin films could be clarified using a Si substrate whose hardness lies between those of TiN (200) and (111). It

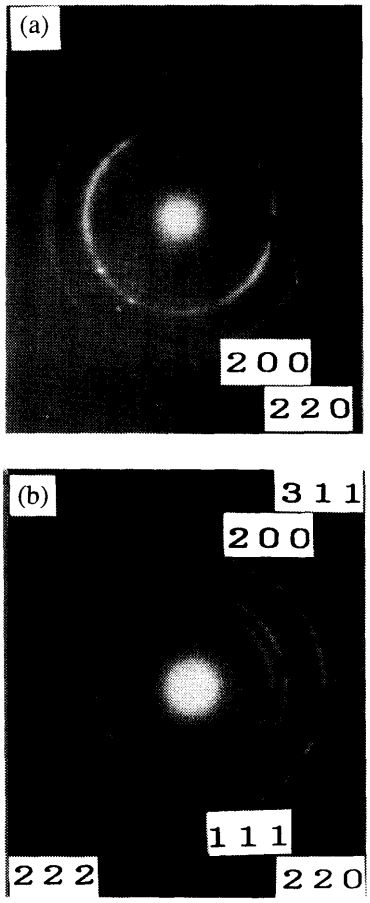

Fig. 3 Diffraction patterns of TiN (200) thin film. (a) is the pattern measured at the periphery of the imprint. (b) is the pattern measured at the center of the imprint

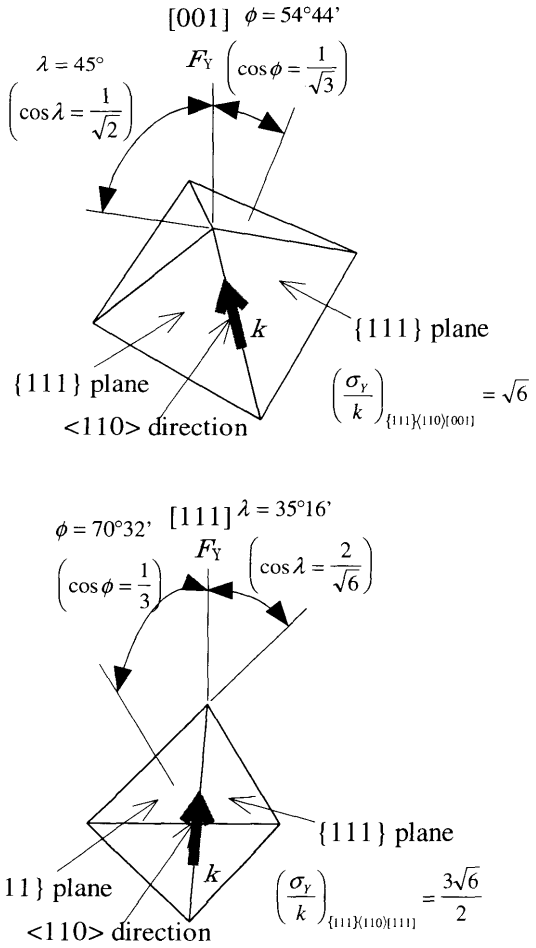

Fig. 4 Equally stressed systems upon pulling along [001] and [111][9]

was confirmed that plastic deformation in TiN thin films occurred irrespective of the preferred orientation.

3.3 Slip system

Our next consideration was the slip system of TiN crystals. Generally, a plastic slip of NaCl-type crystals occurs along the <110> direction[2]. On the other hand, the slip plane of these crystals differed as follows: PbS and PbTe slipped on the {100} plane, while LiF, MgO, and NaCl slipped on the {110} plane[2]. The dominant slip plane of TiN crystals is probably one of {100}, {110} or {111} because of their cubic structure. In this study, the relative strength σ_Y/k, which was the ratio of the yield strength σ_Y to the critically resolved shear stress k, was calculated using Schmid's law for the following hypothetical slip systems, i.e., {100} <110>, {110} <110> and {111} <110>, and was compared to actual hardness anisotropy. Assuming the above discussion to be the case, the initiation and termination of slip deformation were thought to follow Schmid's law. The relative strength σ_Y/k was geometrically determined from the two angles of ϕ and λ from Fig. 4[9], and is shown in Table 4. Here, ϕ is defined as the angle between the normal of the slip plane and the tensile direction, and λ is defined as that between the slip direction and the tensile direction. The ratio of yield strengths of [001] and [111] directions $\sigma_{Y[001]} : \sigma_{Y[111]}$ is also listed in Table 4.

The assumed yield stress σ_Y under consideration in relation to Schmid's law is uniaxial, while the compressive stress during nano-indentation is multiaxial. However, dominant stress, which affects yield strength during the deformation process of the nano-indentation technique, acts along the indentation direction[13]. Therefore, qualitative comparison between uniaxial yield stress σ_Y and experimentally measured hardness is appropriate. On the other hand, Schmid's law is reliable for the antecedent of a single crystal, while actual TiN is a polycrystal. However, the relative strength σ_Y/k under consideration using Schmid's law is constant throughout normal axial rotation. In this study, the TiN film was revealed by XRD analysis to be a normal-axis symmetrical polycrystal with preferred orientation. Therefore, the

Table 4 Relative strength σ_Y/k determined using Schmid's law for three different slip systems[9]

Slip system	[001] direction			[111] direction			$\sigma_{Y[001]}$: $\sigma_{Y[111]}$
	$\cos\phi$	$\cos\lambda$	σ_Y/k	$\cos\phi$	$\cos\lambda$	σ_Y/k	
{111}<110>	$\frac{1}{\sqrt{3}}$	$\frac{1}{\sqrt{2}}$	$\sqrt{6}$	$\frac{1}{3}$	$\frac{2}{\sqrt{6}}$	$\frac{3\sqrt{6}}{2}$	0.67 : 1
{110}<110>	$\frac{1}{\sqrt{2}}$	$\frac{1}{\sqrt{2}}$	2	0	$\frac{2}{\sqrt{6}}$	∞	1 : ∞
{100}<110>	0	$\frac{1}{\sqrt{2}}$	∞	$\frac{1}{\sqrt{3}}$	$\frac{2}{\sqrt{6}}$	$\frac{3\sqrt{2}}{2}$	∞ : 1

application of Schmid's law to preferentially oriented TiN films was valid.

The calculated $\sigma_{Y[001]}$: $\sigma_{Y[111]}$ values differed among the three hypothetical slip systems, as listed in Table 4. In some cases, relative strength σ_Y/k became infinity when cos ϕ value was 0, because slip deformation could not occur in a hypothetical tensile direction. On the other hand, the ratio of experimentally measured hardness $H_{(200)}$: $H_{(111)}$ was 1.67 : 1, as shown in Table 2. These results suggested that the slip system without contradiction was only {100} <110> on the assumption that the ratio of theoretical yield stress $\sigma_{Y[001]}$: $\sigma_{Y[111]}$ was reflected in the ratio of measured hardness $H_{(200)}$: $H_{(111)}$. However, the deformation process during indentation was affected not only by dominant yield stress which acted along an indentation direction but also by other kinds of stress. Therefore, the ratio of experimental $H_{(200)}$: $H_{(111)}$ became a finite value.

It follows from the above discussion that the dominant slip system of TiN crystals is {100} <110>.

3.4 Fracture mechanism

Brittle cracks were produced around the indented depression, as shown in Fig. 2. In this study, the fracture mechanism of TiN thin film during nano-indentation was considered by detailed TEM observation of these cracks.

Figure 5 shows TEM images of brittle cracks in TiN (200) thin film on the Si substrate. This film was indented with load of 500 mN. In this figure, the fracture surface that showed obvious roughness corresponded to the grain boundary, and no cleavage was observed. This suggested that the brittle fracture mechanism of TiN films was not a cleavage fracture but an intergranular fracture.

4. Conclusions

In the present study, (111)- and (200)-oriented TiN thin films prepared by IBAD were indented using a nano-indentation technique. Plastic deformation and brittle fracture of these films were examined based on the results of indentation.

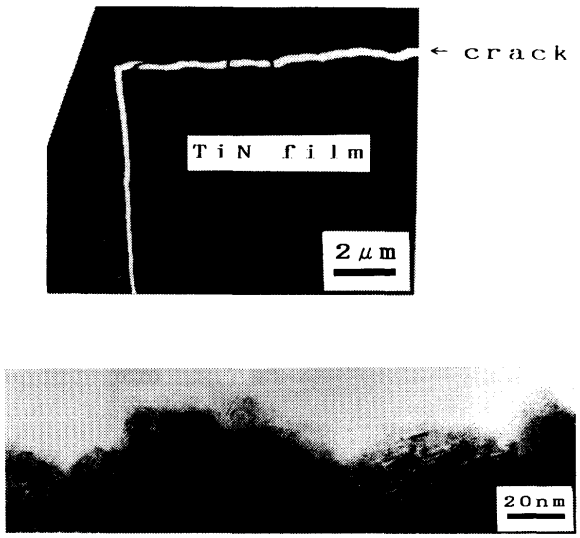

Fig. 5 TEM images of the intergranular fracture in TiN (200) thin film. (a) shows a TEM image, and (b) shows a high-resolution TEM image

(1) Plastic deformation of TiN films occurred during indentation. The deformation of TiN (111) was more obvious than that of TiN (200).

(2) The hardness anisotropy of TiN films was explained by crystallographical anisotropy. The dominant slip system of TiN crystal was suggested to be {100} <110>.

(3) The brittle fracture mechanism of TiN films during nano-indentation was assumed to be not a cleavage fracture but an intergranular fracture.

References

(1) Yamauchi, T., Yamaoka, T., Yashiro, K. and Sobue, S., Effect of Internal Stresses and Microstructure of Sputtered TiN Films on Solid-Phase Reactions with Al-Si-Cu Alloy Films, J. Appl. Phys., Vol. 78, No. 4 (1995), pp. 2385-2391.

(2) Gilman, J.J., Plastic Anisotropy of LiF and Other Rocksalt-Type Crystals, Acta Metallurgica, Vol. 7 (1959), pp. 608-613.

(3) Oh, U.C. and Je, J.H., Effects of Strain Energy on the Preferred Orientation of TiN Thin Films, J. Appl. Phys., Vol. 74, No. 3 (1993), pp. 1692-1696.

(4) Meng, L.-J. and Santos, M.P., Characterization of Titanium Nitride Films Prepared by D.C. Reactive Magnetron Sputtering at Different Nitrogen Pressures, Surf. Coat. Technol., Vol. 90 (1997), pp. 64-70.

(5) Yang, H.H., Je, J.H. and Lee, K.-B., Effect of the Nitrogen Partial Pressure on the Preferred Orientation of TiN Thin Films, J. Mater. Sci. Lett., Vol. 14 (1995), pp. 1635-1637.

(6) Kiuchi, M., Chayahara, A., Horino, Y., Fujii, K. and Satou, M., Control of Preferentially Oriented Crystal Growth of Titanium Nitride, Appl. Surf.

Sci., Vol. 60/61 (1992), pp. 760-764.
(7) Hayashi, T., Matsumuro, A., Muramatsu, M., Kohzaki, M., Takahashi, Y. and Yamaguchi, K., Variation in the Preferred Orientations of TiN Thin Films Prepared by Ion-Beam-Assisted Deposition, J. Jpn. Soc. Prec. Eng., (in Japanese), Vol. 65, No. 9 (1999), pp. 1340-1344.
(8) Matsumuro, A., Watanabe, T., Hayashi, T., Muramatsu, M. and Takahashi, Y., Mechanical Properties of TiN Films with Preferred Orientation by Nano-Indentation Method, J. Soc. Mater. Sci., Jpn., (in Japanese), Vol. 48, No. 12 (1999), pp. 1423-1427.
(9) Backofen, W.A., Deformation Processing (1972), pp. 72-75, Addison-Wesley, Massachusetts.
(10) Müller, P. and Kern, R., About the Measurement of Absolute Isotropic Surface Stress of Crystals, Surf. Sci., Vol. 301 (1994), pp. 386-398.
(11) Samsonov, G.V. and Vinitskii, I.M., Handbook of Chemical Compounds with High Melting Point, (1976), p. 304, Metaddiya, Moscow.
(12) Oettel, H., Bertram, T., Weihnacht, V. and Wiedemann, R., Proc. 5th Int. Symp. on Residual Stress, (1997), pp. 924-930.
(13) Cai, X. and Bangert, H., Hardness Measurements of Thin Films-Determining the Critical Ratio of Depth to Thickness Using FEM, Thin Solid Films, Vol. 264 (1995), pp. 59-71.